Adaptive boundary observer design for linear hyperbolic systems; Application to estimation in heat exchangers

Mohammad Ghousein, Emmanuel Witrant, Viren Bhanot, Paolo Petagna

Version of Record: https://www.sciencedirect.com/science/article/pii/S0005109820300224
Manuscript_f64d618ca647f2b4273c80c6dd75aff0

Adaptive Boundary Observer Design for Linear Hyperbolic Systems; Application to Estimation in Heat Exchangers

Mohammad Ghousein[a], Emmanuel Witrant[a], Viren Bhanot[b], Paolo Petagna[b]

[a] *Univ. Grenoble Alpes, GIPSA-Lab, 11 Rue des Mathématiques 38400 Saint-Martin-d'Hères, France*
[b] *Physics Department (PH), CERN, Route de Meyrin, 1211 Genève, Switzerland*

Abstract

In this work, we consider the estimation of temperature along the pipes of concentric heat exchanger tubes in which CO_2 is the working fluid. The transport phenomena is modeled using (2x2) linear hyperbolic partial differential equations, with one rightward equation for the hot flow and one leftward equation for the cold flow. Both flows exchange energy through the wall interface, which physically induces a coupling between the two dynamics. Our objective is to estimate the temperature distribution along the flows from measurements at the tubes boundaries only. In this framework, we propose an adaptive boundary observer that can estimate not only the full state of the system, but also unknown in-domain parameters. The design is based on transforming the error system via a finite-dimensional backstepping-like transformation into a desired filter-based system, for which standard backstepping observer techniques and adaptation laws can be used. The theoretical results are evaluated against the temperature measurements taken from a CO_2 refrigeration apparatus built at CERN, Switzerland.

Keywords: Boundary Observers, Boundary Control, Fluid dynamics, Hyperbolic partial differential equations, Lyapunov theory, Backstepping boundary estimation, Adaptive state observers

1. Introduction

Heat exchangers are widely used in many industrial domains like food production, chemical plants or oil refineries. They also play an important role for cooling and heating of houses, offices, companies, cars etc. In the past decades fluorocarbons (C_2F_6, C_3F_8, R134a) were used as the working fluids for heat exchangers, but nowadays CO_2 (especially evaporative CO_2) cooling has become an interesting technology due to several advantages. Indeed, CO_2 has high heat transfer capabilities, high latent heat, low pressure drop and low viscosity (ability to use small size pipes), which allows us to cool networks of long small pipes over large distances. CO_2 has thus been retained as the best choice for HEP detectors cooling at CERN [1]. Heat exchangers are key components that are present in any refrigeration system. The control of such units is vital in order to have low rates of energy consumption while maximizing the heat transfer rates. Considering the concentric tubes heat exchanger, both hot and cold fluids exchange energy through the wall interface. This transport and exchange of energy can be modeled by first order linear hyperbolic systems of balance laws [2]. Synthesizing a control law may require a full knowledge of the distributed state while measurements are available only at the tube boundaries. Furthermore, full state knowledge helps in managing energy efficiently in complex and large heat exchanger networks, and to detect faults in case of an energy leakage.

The classical approach used for solving control and estimation problems for hyperbolic partial differential equations is to discretize the partial differential equations (PDEs) and then apply classical control methods designed for finite dimensional systems. However, key information on the system transient behavior is lost, and the observability and controllability of the system will depend on the chosen space-discretization method. This leads to the idea of extending finite dimensional control theory to the infinite case. An extra challenge induced by our estimation problem is the lack of knowledge of some in-domain coupling parameters (e.g. the heat transfer coefficient). This adds more complexity to the estimation problem as we also have unmeasured distributed states. This motivates our work to consider the adaptive design of a boundary observer that can simultaneously estimate the distributed states and the unknown in-domain parameters, with only boundary measurements.

Hyperbolic systems and more specifically linear and quasi-linear hyperbolic systems are well studied by the control community. These systems can model many physical processes, like road traffic [3], gas flow in pipelines [4], flow of fluids in open channels [5], transmission lines

Email addresses: mohammad.ghousein@gipsa-lab.fr (Mohammad Ghousein), emmanuel.witrant@gipsa-lab.fr (Emmanuel Witrant), viren.bhanot@cern.ch (Viren Bhanot), paolo.petagna@cern.ch (Paolo Petagna)

[6], multiphase flow [7], etc.. The early results on stability and controllability of such systems can be dated back to the 70s [8], [9]. During that period, the stability issue was tackled by computing the explicit solution of the equations along the characteristic curves in the framework of the C^1 norm. Afterwards, using Lyapunov-based functions, dissipative boundary conditions (standard static boundary output feedback) are designed to guarantee exponential stability in the L^2, C^1 and H^2 norms [2, 10, 11]. One drawback of using this kind of boundary conditions to stabilize the system is that it imposes some restrictions on the magnitude of the coupling between the system states. However, this limitation can be overcome by the use of the so-called backstepping-method. The main idea of this method is to introduce an invertible Volterra transformation that maps the original system into a target system with the desired stability properties, for which static boundary controls and observer gains are synthesized to ensure the system convergence to a desired set in finite time. In [12], the authors solve the problem of one-sided boundary stabilization (actuation only at one boundary) of a two by two quasilinear first-order hyperbolic system in finite time. The approach is then generalized by the authors in [13] to a general system of heterodirectional coupled hyperbolic equations. The backstepping method is also used for two-sided boundary control (actuation on both boundaries) of heterodirectional hyperbolic systems. The authors in [14] derive control laws using a Fredholm transformation (unlike Volterra transformation, Fredholm transformation is not always invertible) that also ensures convergence in finite time. However, all the results mentioned so far do not allow unknown in-domain parameters or unknown boundary parameters to be present. In order to address this problem, we consider adaptive boundary control for hyperbolic systems. The first results on adaptive control for hyperbolic PDEs were obtained by the authors in [15], where a general first-order hyperbolic partial integro-differential equation(PIDE) with one rightward convecting PDE is adaptively stabilized by boundary sensing only. This result is extended by the authors in [16] to 2 by 2 hyperbolic partial differential equations with unknown transport speeds, unknown couplings and also unknown boundary parameters.

Infinite dimensional boundary observers are less investigated in the literature. The problem with systems that have distributed parameters is that it is most of the time impossible to take measurements at every point in space. It is more natural for the sensors to be located at the boundaries of the domain, which led to the idea of boundary observers. Boundary control design is achieved using boundary observers based on two methods: Lyapunov and backstepping-based methods. Concerning Lyapunov methods, the authors in [17] design a boundary observer for n rightward hyperbolic transport equations. The observer uses measurements taken from the right boundary to correct the estimation error on the left one. This result is extended by the authors in [18] to one rightward and one leftward transport equation for the plate heat exchanger. Nevertheless, both methods assume perfect knowledge of the model parameters. Backstepping-based boundary observers are also well established in the literature. In fact, static control design using backstepping requires a full knowledge of the distributed states. A collocated boundary observer is thus synthesized to fulfill this requirement (see previously mentioned results such as [12],[13],[14]). These designs also assume a perfect knowledge of the system. In many practical cases, some model parameters are unknown, which motivates the need for adaptive estimators.
The objective of an adaptive boundary observer is to simultaneously construct the system's distributed states and the unknown parameters from only boundary sensing. The problem of adaptive boundary estimation was first addressed by the authors in [19] for parabolic PDEs using backstepping techniques. Such method is applied to hyperbolic systems in [20], where the authors design an adaptive observer for first-order hyperbolic systems with uncertain additive boundary parameters (the adaptive laws for these parameters are derived using Lyapunov analysis). This result is extended by the authors in [21] to unknown additive and multiplicative parameters in the boundary. We can also mention the results on disturbance rejection for hyperbolic systems (see e.g. [22], [23]), which can be interpreted as results on adaptive observers for hyperbolic PDEs. As a different approach, swapping design is also used in the derivation of adaptive observers. This method relies on using K-filters to derive static relationships between the system states and the unknown parameters: this relationship is used to build Lyapunov-based adaptive laws to estimate the unknown parameters (see [24] and [25] for ODEs and [19] for PDEs). In the work of the authors in [26], [27], and [28] swapping design is used to estimate unknown boundary parameters for some classes of hyperbolic systems. However, few results exist in the literature on in-domain parameter estimation. The works [15] and [16] on adaptive control include in-domain parameter estimations based on swapping design methods. In these works, an adaptive observer is designed for systems in the "canonical observable form" to serve as an intermediate step in deriving the control law. In this paper, we consider the problem of estimating the distributed states of a 2×2 hyperbolic system, two-sided actuated with unknwon in- domain parameters. The motivation behind considering such system is the application to heat exchanger networks. To the best of our knowledge, this type of estimation problem is not addressed yet in the literature. Inspired by [29], the novelty of our adaptive design is to apply the swapping method on the error estimation system and not on the original plant. This gives more degrees of freedom for the designer to shape the boundary conditions of the resulting error system, which facilitates the use of a

backstepping technique to derive the observer gains. In addition, we validate the proposed adaptive architecture experimentally using temperature measurements taken from a CO_2 refrigeration apparatus built at CERN.
The paper is organized as follows: the observation problem formulation is described in Section 2. The adaptive observer design with the estimation convergence analysis is presented in Section 3. Section 4 is dedicated to the experimental setup together with the experimental evaluation results, and some concluding remarks are given in Section 5.

2. Observation problem formulation

We consider the following class of linear hyperbolic systems evolving in $\{(t,x) \mid t \geq 0, x \in [\,0,1\,]\}$:

$$\partial_t u + c_1 \partial_x u = \sigma_1(x) v + \theta_1 \phi_1(x,t) \tag{1}$$

$$\partial_t v - c_2 \partial_x v = \sigma_2(x) u + \theta_2 \phi_2(x,t) \tag{2}$$

$$u(0,t) = U(t), \quad v(1,t) = V(t) \tag{3}$$

where u and v are the system states, $[\,u,v\,]^T : [\,0,1\,] \times [\,0,+\infty) \to \mathbb{R}^2$. $c_1 > 0$ and $c_2 > 0$ are the transport speeds, and σ_1, σ_2 are assumed to be $C^0([0,1];\mathbb{R})$ known functions. Furthermore, ϕ_1 and ϕ_2 are also bounded known functions of class $C^1([\,0,1\,] \times [\,0,+\infty);\mathbb{R})$, and θ_1 and θ_2 are unknown real scalar parameters. The initial conditions, denoted u_0 and v_0, are assumed to belong to $L^2([0,1])$. $U(t)$ and $V(t)$ are considered as known boundary inputs.
Our goal is to estimate the state of the system (1)-(3) and the unknown parameters θ_1 and θ_2, assuming that the following measurements are available:

$$y_1(t) = u(1,t), \quad y_2(t) = v(0,t) \tag{4}$$

Remark 1. *While the method extends to spatially varying transport speeds $c_1(x)$ and $c_2(x)$, we consider here constant transport speeds for the sake of technical simplicity.*

Remark 2. *The method can be extended to include the estimation of unknown boundary parameters of the form $u(0,t) = qv(0,t) + U(t)$ where q is the unknown boundary parameter. Nevertheless, this requires assuming that the plant is stable and does not diverge for all times.*

3. Adaptive Observer Design

We introduce the following adaptive observer design:

$$\partial_t \hat{u} + c_1 \partial_x \hat{u} = \sigma_1(x)\hat{v} + \hat{\theta}_1(t)\phi_1(x,t) - p_1(x)(\hat{u}(1,t) - y_1(t)) + m_1(x,t) \tag{5}$$

$$\partial_t \hat{v} - c_2 \partial_x \hat{v} = \sigma_2(x)\hat{u} + \hat{\theta}_2(t)\phi_2(x,t) - p_2(x)(\hat{u}(1,t) - y_1(t)) + m_2(x,t) \tag{6}$$

$$\hat{u}(0,t) = U(t) + q(\hat{v}(0,t) - y_2(t)) \tag{7}$$

$$\hat{v}(1,t) = V(t) \tag{8}$$

where $p_1(x)$ and $p_2(x)$ are the observer gains, q is a non-zero real parameter that can be chosen arbitrarily, and $m_1(x,t)$ and $m_2(x,t)$ are additional feedback gains to be determined later. The observer initial conditions are denoted by $\hat{u}_0$ and $\hat{v}_0$, and are assumed to belong to $L^2[0,1]$. The estimates are denoted by hat, and we define the error variables $\tilde{u} = u - \hat{u}$, $\tilde{v} = v - \hat{v}$, $\tilde{\theta}_1(t) = \theta_1 - \hat{\theta}_1(t)$, $\tilde{\theta}_2(t) = \theta_2 - \hat{\theta}_2(t)$.
Forming the error system by subtracting (5)-(8) from (1)-(3) we have:

$$\partial_t \tilde{u} + c_1 \partial_x \tilde{u} = \sigma_1(x)\tilde{v} + \tilde{\theta}_1(t)\phi_1(x,t) - p_1(x)\tilde{u}(1,t) - m_1(x,t) \tag{9}$$

$$\partial_t \tilde{v} - c_2 \partial_x \tilde{v} = \sigma_2(x)\tilde{u} + \tilde{\theta}_2(t)\phi_2(x,t) - p_2(x)\tilde{u}(1,t) - m_2(x,t) \tag{10}$$

$$\tilde{u}(0,t) = q\tilde{v}(0,t), \quad \tilde{v}(1,t) = 0 \tag{11}$$

The observer designed in (5)-(8) is a Luenberger-type observer, which is a copy of the system with output injection terms $(y_1(t), y_2(t))$ added in the domain and at the left boundary. The problem is then to find the observer gains $p_1(x)$ and $p_2(x)$, and proper parameter update laws in order to guarantee the exponential convergence of the error system (9)-(11) to zero.

3.1. Swapping Design

In this section, we derive a static relationship which connects the estimation error on the states with the estimation error on the parameters. This relationship will then be used to derive the parameters adaption laws. By writing the error system (9)-(11) using swapping filters we have:

$$z_1(x,t) = \tilde{u}(x,t) - \lambda_{11}(x,t)\tilde{\theta}_1(t) - \lambda_{12}(x,t)\tilde{\theta}_2(t) \tag{12}$$

$$z_2(x,t) = \tilde{v}(x,t) - \lambda_{21}(x,t)\tilde{\theta}_1(t) - \lambda_{22}(x,t)\tilde{\theta}_2(t) \tag{13}$$

We can write (12)-(13) in the compact form:

$$Z(x,t) = E(x,t) - \Lambda(x,t)\tilde{\theta}(t) \tag{14}$$

where:

$$Z(x,t) = \begin{pmatrix} z_1(x,t) \\ z_2(x,t) \end{pmatrix}, \quad E(x,t) = \begin{pmatrix} \tilde{u}(x,t) \\ \tilde{v}(x,t) \end{pmatrix}$$

$$\tilde{\theta}(t) = \begin{pmatrix} \tilde{\theta}_1(t) \\ \tilde{\theta}_2(t) \end{pmatrix}, \quad \Lambda(x,t) = \begin{bmatrix} \lambda_{11}(x,t) & \lambda_{12}(x,t) \\ \lambda_{21}(x,t) & \lambda_{22}(x,t) \end{bmatrix}$$

The swapping filters $\lambda_{ij}(x,t) : [0,1] \times [0,+\infty) \to \mathbb{R}$, $(1 \leq i \leq 2, 1 \leq j \leq 2)$ are to be defined later. Differentiating (12) with respect to time and substituting with (9) we get:

$$\partial_t z_1 = -c_1 \partial_x \tilde{u} + \sigma_1(x)\tilde{v} + \dot{\tilde{\theta}}_1(t)\phi_1(x,t) - m_1(x,t) - p_1(x)\tilde{u}(1,t) - \partial_t \lambda_{11}\tilde{\theta}_1 - \lambda_{11}\dot{\tilde{\theta}}_1 - \partial_t \lambda_{12}\tilde{\theta}_2 - \lambda_{12}\dot{\tilde{\theta}}_2 \quad (15)$$

In order to keep (15) linear in $\tilde{\theta}_1$ and $\tilde{\theta}_2$, we choose the following feedback law $m_1(x,t)$:

$$m_1(x,t) = -\lambda_{11}(x,t)\dot{\tilde{\theta}}_1(t) - \lambda_{12}(x,t)\dot{\tilde{\theta}}_2(t) \quad (16)$$

Using (16), and substituting with (14) in (15) leads to:

$$\begin{aligned}\partial_t z_1 + c_1 \partial_x z_1 &= \sigma_1(x) z_2 - p_1(x) z_1(1,t) \\ &+ \tilde{\theta}_1(-\partial_t \lambda_{11} - c_1 \partial_x \lambda_{11} + \sigma_1(x)\lambda_{21} - p_1(x)\lambda_{11}(1,t) + \phi_1(x,t)) \\ &+ \tilde{\theta}_2(-\partial_t \lambda_{12} - c_1 \partial_x \lambda_{12} + \sigma_1(x)\lambda_{22} - p_1(x)\lambda_{12}(1,t))\end{aligned} \quad (17)$$

Similarly, deriving (13) with respect to time and following the same procedure, one gets:

$$m_2(x,t) = -\lambda_{21}(x,t)\dot{\tilde{\theta}}_1(t) - \lambda_{22}(x,t)\dot{\tilde{\theta}}_2(t) \quad (18)$$

$$\begin{aligned}\partial_t z_2 - c_2 \partial_x z_2 &= \sigma_2(x) z_1 - p_2(x) z_1(1,t) \\ &+ \tilde{\theta}_1(-\partial_t \lambda_{21} + c_2 \partial_x \lambda_{21} + \sigma_2(x)\lambda_{11} - p_2(x)\lambda_{11}(1,t)) \\ &+ \tilde{\theta}_2(-\partial_t \lambda_{22} + c_2 \partial_x \lambda_{22} + \sigma_2(x)\lambda_{12} - p_2(x)\lambda_{12}(1,t) + \phi_2(x,t)))\end{aligned} \quad (19)$$

Equations (17) and (19) suggest the following dynamics of the swapping filters:

$$\partial_t \lambda_{11} + c_1 \partial_x \lambda_{11} = \sigma_1(x)\lambda_{21} - p_1(x)\lambda_{11}(1,t) + \phi_1(x,t) \quad (20)$$

$$\partial_t \lambda_{21} - c_2 \partial_x \lambda_{21} = \sigma_2(x)\lambda_{11} - p_2(x)\lambda_{11}(1,t) \quad (21)$$

$$\partial_t \lambda_{12} + c_1 \partial_x \lambda_{12} = \sigma_1(x)\lambda_{22} - p_1(x)\lambda_{12}(1,t) \quad (22)$$

$$\partial_t \lambda_{22} - c_2 \partial_x \lambda_{22} = \sigma_2(x)\lambda_{12} - p_2(x)\lambda_{12}(1,t) + \phi_2(x,t) \quad (23)$$

and we impose the following boundary conditions:

$$\lambda_{11}(0,t) = q\lambda_{21}(0,t), \quad \lambda_{21}(1,t) = 0 \quad (24)$$

$$\lambda_{12}(0,t) = q\lambda_{22}(0,t), \quad \lambda_{22}(1,t) = 0 \quad (25)$$

with zero distributed initial conditions $\Lambda(x,0) = 0$. It is important to notice that the system (20)-(21) with boundary conditions (24), and the system (22)-(23) with boundary conditions (25) are independent of each other. Hence, we can denote by:

$$\Lambda_1(x,t) = \begin{pmatrix} \lambda_{11}(x,t) \\ \lambda_{21}(x,t) \end{pmatrix}, \quad \Lambda_2(x,t) = \begin{pmatrix} \lambda_{12}(x,t) \\ \lambda_{22}(x,t) \end{pmatrix} \quad (26)$$

two separate subsystems of $\Lambda(x,t)$. Doing so, and substituting equations (20)-(23) in (17) and (19), the dynamics of the transformed state $Z(x,t)$ becomes

$$\partial_t z_1 + c_1 \partial_x z_1 = \sigma_1(x) z_2 - p_1(x) z_1(1,t) \quad (27)$$

$$\partial_t z_2 - c_2 \partial_x z_2 = \sigma_2(x) z_1 - p_2(x) z_1(1,t) \quad (28)$$

Also, using the boundary conditions given in (11), (24) and (25), we can then derive the boundary conditions of $Z(x,t)$ using transformation (14) as:

$$z_1(0,t) = q z_2(0,t), \quad z_2(1,t) = 0 \quad (29)$$

In view of the transformation (14), the state estimation error $E(x,t)$ splits into two parts. The first component is the observation error represented by $Z(x,t)$, which is always present whether we have parameters to estimate or not. The second component is the parameter-induced error represented by $\Lambda(x,t)\tilde{\theta}(t)$, which is proportional to the parameters mismatch. It is important to mention that the idea of state parametrization was was first introduced by the authors in [25] for ODEs. To sum up, the problem of the exponential stability of the error system (9)-(11) is equivalent to address three problems: the exponential stability of $Z(x,t)$, the exponential stability of $\tilde{\theta}(t)$ and the boundedness of $\Lambda(x,t)$.

3.2. Exponential stability of Z(x,t)

We start our analysis by considering the $Z(x,t)$ system (27)-(29) our goal is to select the observer gains $p_1(x)$ and $p_2(x)$ such that the equilibrium $z_1 \equiv z_2 \equiv 0$ is exponentially stable in the L^2 sense. In fact, equation (14) allows a straightforward application of the results in [12] (section 4). The authors use a Volterra-backstepping transformation of the second kind to map the system (27)-(29) into an exponentially stable target system. We present here the transformation for the sake of completeness:

$$Z(x,t) = \tilde{\gamma}(x,t) - \int_x^1 P(x,\xi)\tilde{\gamma}(\xi,t)d\xi \quad (30)$$

$$\begin{aligned} P(x,\xi) &= \begin{pmatrix} P^{11}(x,\xi) & P^{12}(x,\xi) \\ P^{21}(x,\xi) & P^{22}(x,\xi) \end{pmatrix}, \\ \tilde{\gamma}(x,t) &= \begin{pmatrix} \tilde{\alpha}(x,t) \\ \tilde{\beta}(x,t) \end{pmatrix} \end{aligned} \quad (31)$$

The transformation evolves in the triangular domain $\mathrm{L} = \{(x,\xi), 0 \leq x \leq \xi \leq 1\}$, and maps the $Z(x,t)$ system (27)-(29) into the target system $\tilde{\gamma}(x,t)$ given by:

$$\partial_t \alpha + c_1 \partial_x \alpha = 0 \quad (32)$$

$$\partial_t \beta - c_2 \partial_x \beta = 0 \quad (33)$$

$$\alpha(0,t) = q\beta(0,t), \quad \beta(1,t) = 0 \quad (34)$$

To achieve this transformation, the kernel equations must satisfy the following equations:

$$c_1 P^{11}_x + c_1 P^{11}_\xi = \sigma_1(x) P^{21} \tag{35}$$

$$c_1 P^{12}_x - c_2 P^{12}_\xi = \sigma_1(x) P^{22} \tag{36}$$

$$c_2 P^{21}_x - c_1 P^{21}_\xi = -\sigma_2(x) P^{11} \tag{37}$$

$$c_2 P^{22}_x + c_2 P^{22}_\xi = -\sigma_2(x) P^{12} \tag{38}$$

with boundary conditions:

$$P^{11}(0,\xi) = qP^{21}(0,\xi), \quad P^{12}(x,x) = \frac{\sigma_1(x)}{c_1+c_2} \tag{39}$$

$$P^{21}(x,x) = -\frac{\sigma_2(x)}{c_1+c_2}, \quad P^{22}(0,\xi) = \frac{1}{q} P^{12}(0,\xi) \tag{40}$$

The observer gains $p_1(x)$ and $p_2(x)$ serve as additional conditions on the output injection kernels as:

$$p_1(x) = -c_1 P^{11}(x,1), \quad p_2(x) = -c_2 P^{21}(x,1) \tag{41}$$

It has been shown in [12] that the kernel equations (35)-(40) have a unique solution in $C(Ł)$ and are invertible. The inverse transformation is denoted by $R(x,\xi)$ and is given by:

$$\tilde{\gamma}(x,t) = Z(x,t) + \int_x^1 R(x,\xi) Z(\xi,t) d\xi \tag{42}$$

$$R(x,\xi) = \begin{pmatrix} R^{11}(x,\xi) & R^{12}(x,\xi) \\ R^{21}(x,\xi) & R^{22}(x,\xi) \end{pmatrix}, \tag{43}$$

with the following kernel equations:

$$c_1 R^{11}_x + c_1 R^{11}_\xi = -\sigma_2(\xi) R^{12} \tag{44}$$

$$c_1 R^{12}_x - c_2 R^{12}_\xi = -\sigma_1(\xi) R^{11} \tag{45}$$

$$c_2 R^{21}_x - c_1 R^{21}_\xi = \sigma_2(\xi) R^{22} \tag{46}$$

$$c_2 R^{22}_x + c_2 R^{22}_\xi = \sigma_1(\xi) R^{21} \tag{47}$$

with boundary conditions:

$$R^{11}(0,\xi) = qR^{21}(0,\xi), \quad R^{12}(x,x) = \frac{\sigma_1(x)}{c_1+c_2} \tag{48}$$

$$R^{21}(x,x) = -\frac{\sigma_2(x)}{c_1+c_2}, \quad R^{22}(0,\xi) = \frac{1}{q} R^{12}(0,\xi) \tag{49}$$

In fact, using a quadratic Lyapunov function and the method of characteristics, on can easily show that $\tilde{\gamma}(x,t)$ is L^2 stable and that $\alpha \equiv \beta \equiv 0$ is reached in finite time for all $0 \leq x \leq 1$. Referring back to (30) and (42), the stability properties of the $\tilde{\gamma}(x,t)$ and $Z(x,t)$ are equivalent. The following Theorem (which is Theorem 2 in [12]) states the stability results for the $Z(x,t)$ system.

Theorem 1 ([12]). *Consider the system (27)-(28) with boundary conditions (29), initial conditions z_1^0, z_2^0 in $L^2[0,1]$ and with observer gains (41). The equilibrium $z_1 \equiv z_2 \equiv 0$ is exponentially stable in the L^2 sense, and the equilbrium is reached in finite time $t_F = \frac{1}{c_1} + \frac{1}{c_2}$.*

Remark 3. *The convergence of $Z(x,t)$ to zero in a finite time is independent of the parameter update laws.*

3.3. Boundedness of $\Lambda(x,t)$

In this section, we prove the boundedness of the swapping filters $\Lambda(x,t)$ in the L^2 sense. This is necessary, as introduced in Section 3.1 and shown in Section 3.5, to conclude on the exponential stability of $E(x,t)$.

Theorem 2. *Consider the two subsystems $\Lambda_1(x,t)$ and $\Lambda_2(x,t)$ with the initial conditions $\Lambda_1(x,0), \Lambda_2(x,0) \in L^2[0,1]$, the observer gains (41), and with ϕ_1 and ϕ_2 two bounded functions of class $C^1([0,1] \times [0,+\infty); \mathbb{R})$. Then we have that $||\Lambda_1(.,t)||_{L^2[0,1]}$ and $||\Lambda_2(.,t)||_{L^2[0,1]}$ are bounded.*

PROOF. First, consider $\Lambda_1(x,t)$. It's clear that this system has exactly the same shape as the $Z(x,t)$ system with the addition of the bounded function $\phi_1(x,t)$ in the spatial domain. As a result, it's easy to check that the same transformation $R(x,\xi)$ defined by equations (44)-(49) maps $\Lambda_1(x,t)$ to the following target system:

$$\Delta(x,t) = \Lambda_1(x,t) + \int_x^1 R(x,\xi) \Lambda_1(\xi,t) d\xi \tag{50}$$

$$\Delta(x,t) = \begin{pmatrix} a(x,t) \\ b(x,t) \end{pmatrix} \tag{51}$$

where the dynamics of $\Delta(x,t)$ is given by:

$$\partial_t a + c_1 \partial_x a = f_1(x,t) \tag{52}$$

$$\partial_t b - c_2 \partial_x b = f_2(x,t) \tag{53}$$

$$a(0,t) = qb(0,t), \quad b(1,t) = 0 \tag{54}$$

where $f_1(x,t) = \phi_1(x,t) + \int_x^1 R^{11}(x,\xi)\phi_1(\xi,t)d\xi$ and $f_2(x,t) = \int_x^1 R^{21}(x,\xi)\phi_1(\xi,t)d\xi$. We recall that $R(x,\xi)$ is well-defined and continuous on $C(Ł)$ (see [12]): thus $R(x,\xi)$ is also bounded on $C(Ł)$. By the assumption that $\phi_1(x,t)$ is bounded, we can conclude that the two functions $f_1(x,t)$ and $f_2(x,t)$ are also bounded on $\{(t,x) \mid t \geq 0, x \in [0,1]\}$. Now consider the following Lyapunov function:

$$V_1(t) = \frac{1}{2} \int_0^1 \frac{q_1}{c_1} e^{-\mu x} a^2(x,t) + \frac{q_2}{c_2} e^{\mu x} b^2(x,t) dx \tag{55}$$

where q_1, q_2 and μ are positive constants. Taking the time derivative of (55) we get:

$$\dot{V}_1(t) = \int_0^1 \frac{q_1}{c_1} e^{-\mu x} a \partial_t a + \frac{q_2}{c_2} e^{\mu x} b \partial_t b \, dx \tag{56}$$

Using (52)-(54) and integrating by parts, one has:

$$\begin{aligned}\dot{V}_1(t) = &-\frac{1}{2}q_1 e^{-\mu}a^2(1,t) + \frac{1}{2}(q_1 q^2 - q_2)b^2(0,t) \\ &- \frac{\mu}{2}\int_0^1 q_1 e^{-\mu x}a^2(x,t) + q_2 e^{\mu x}b^2(x,t)dx \\ &+ \int_0^1 \frac{q_1}{c_1}e^{-\mu x}f_1(x,t)a(x,t) + \frac{q_2}{c_2}e^{\mu x}f_2(x,t)b(x,t)dx\end{aligned} \tag{57}$$

Applying Young's inequality to the last term of (57), we have, for all $k_1 > 0, k_2 > 0$, that:

$$\begin{aligned}\dot{V}_1(t) \leq &-\frac{1}{2}q_1 e^{-\mu}a^2(1,t) + \frac{1}{2}(q_1 q^2 - p_2)b^2(0,t) \\ &+ (-\frac{\mu}{2} + \frac{k_1}{2c_1})\int_0^1 q_1 e^{-\mu x}a^2(x,t)dx \\ &+ (-\frac{\mu}{2} + \frac{k_2}{2c_2})\int_0^1 q_2 e^{\mu x}b^2(x,t)dx \\ &+ \frac{1}{2k_1}\int_0^1 \frac{q_1}{c_1}e^{-\mu x}f_1^2(x,t)dx \\ &+ \frac{1}{2k_2}\int_0^1 \frac{q_2}{c_2}e^{\mu x}f_2^2(x,t)dx\end{aligned} \tag{58}$$

We can choose $\mu = 1$, and q_1 and q_2 such that:

$$q_1 q^2 - q_2 \leq 0 \tag{59}$$

Let $\Gamma \in]0, min\{c_1, c_2\}[$, $k_1 \in]0, c_1 - \Gamma]$ and $k_2 \in]0, c_2 - \Gamma]$, then we have

$$\begin{aligned}&\dot{V}_1(t) \leq -\Gamma V_1(t) + \\ &\frac{1}{2k_1}\int_0^1 \frac{q_1}{c_1}e^{-\mu x}f_1^2(x,t)dx + \frac{1}{2k_2}\int_0^1 \frac{q_2}{c_2}e^{\mu x}f_2^2(x,t)dx\end{aligned} \tag{60}$$

It follows from (60) that $V_1(t)$ is bounded, as a direct consequence of the boundedness of $f_1(x,t)$ and $f_2(x,t)$. Since $V_1(t)$ serves as the weighted L^2 norm of the $\Delta(x,t)$ system and since the transformation $R(x,\xi)$ is invertible, we can deduce that $||\Lambda_1(.,t)||_{L^2[0,1]}$ is bounded and the proof is complete.
The boundedness of $||\Lambda_2(.,t)||_{L^2[0,1]}$ is done in exactly the same way, since the two systems are symmetric.

3.4. Parameter adaptation laws and exponential stability of $\tilde{\theta}(t)$

The authors in [30] synthesize adaptation laws for static regressors equations of this general from:

$$y(t) = \phi^T(t)\theta \tag{61}$$

where y is the vector of outputs, ϕ is the regressor and θ is the vector of unknown parameters. The core of the designs is based on minimizing cost functions of the squared estimation errors. Then, sufficient conditions for the exponential convergence of the estimates are given using Lyapunov analysis considering persistent excitation assumptions. In this section, we adapt the analysis of [30] to synthesize an adaptive law for our problem and prove that $\hat{\theta}(t) \to \theta$ exponentially fast.
In view of the available measurements given in (4), equations (12) and (13) are evaluated at $x = 1$ and $x = 0$, respectively, and we have that:

$$Z_p(t) = E_p(t) - \Lambda_p(t)\tilde{\theta}(t) \tag{62}$$

where:

$$Z_p(t) = \begin{pmatrix} z_1(1,t) \\ z_2(0,t) \end{pmatrix}, \quad E_p(t) = \begin{pmatrix} \tilde{u}(1,t) \\ \tilde{v}(0,t) \end{pmatrix}$$
$$\Lambda_p(t) = \begin{bmatrix} \lambda_{11}(1,t) & \lambda_{12}(1,t) \\ \lambda_{21}(0,t) & \lambda_{22}(0,t) \end{bmatrix}$$

Equation (62) has a form similar to (61) and suggests the following normalized parameter adaptation law (continuous-time recursive least squares estimator with a forgetting factor):

$$\dot{\hat{\theta}}(t) = s(t)\frac{P(t)\Lambda_p^T}{1 + ||\Lambda_p^T\Lambda_p||^2}E_p(t), \tag{63}$$

$$\dot{P}(t) = s(t)\left[\beta P(t) - \frac{P(t)\Lambda_p^T\Lambda_p P(t)}{1 + ||\Lambda_p^T\Lambda_p||^2}\right], \tag{64}$$

$$s(t) = \begin{cases} 1 & if \quad t > t_F \\ 0 & else \end{cases} \tag{65}$$

where $\hat{\theta}(t)$ is the estimated value of θ, $P(t) \in \mathbb{R}^{2\times 2}$, and $\beta > 0$ is the forgetting factor. The initial conditions $\hat{\theta}(0) = \hat{\theta}_0$, and $P(0) = P_0 = P_0^T > 0$ are chosen arbitrarily.
To prove that $\hat{\theta}(t) \to \theta$ exponentially fast, we assume the following:

Assumption 1. *We assume that $\Lambda_p(t)$ is persistently exciting i.e. for all $t \geq 0$ there exist positive constants T_0, c_0 and c_1 so that:*

$$c_0 I \leq \frac{1}{T_0}\int_t^{t+T_0} \Lambda_p^T(\tau)\Lambda_p(\tau)d\tau \leq c_1 I \tag{66}$$

where $I \in \mathbb{R}^{2\times 2}$ denotes the identity matrix. The convergence of the estimate $\hat{\theta}(t)$ is then given by the following Theorem.

Theorem 3. *Consider the system (63)-(65) with initial conditions given by $\hat{\theta}_0$ and P_0. Using Theorems 1 and 2, and assuming that (66) holds, then $\hat{\theta}(t) \to \theta$ exponentially fast.*

PROOF. First, we compute the dynamics of the estimation error on $\tilde{\theta}(t)$ using (14) and (63) as:

$$\begin{aligned}\dot{\tilde{\theta}}(t) = -\dot{\hat{\theta}} &= -s(t)\frac{P(t)\Lambda_p^T}{1 + ||\Lambda_p^T\Lambda_p||^2}E_p(t) \\ &= -s(t)\frac{P(t)\Lambda_p^T}{1 + ||\Lambda_p^T\Lambda_p||^2}Z_p(t) - s(t)\frac{P(t)\Lambda_p^T\Lambda_p}{1 + ||\Lambda_p^T\Lambda_p||^2}\tilde{\theta}(t)\end{aligned} \tag{67}$$

it's also easy to check that (64) is equivalent to

$$\frac{d}{dt}(P^{-1}) = s(t)\left[-\beta P^{-1} + \frac{\Lambda_p^T \Lambda_p}{1+||\Lambda_p^T \Lambda_p||^2}\right] \tag{68}$$

where $P^{-1}(t) \in \mathbb{R}^{2\times 2}$ is the inverse matrix of $P(t)$. It can be shown (see e.g. [30]), under Assumption 1, that $P^{-1}(t)$ is positive definite and bounded. Now, we can define the following Lyapunov function:

$$V(t) = \frac{1}{2}\tilde{\theta}^T(t)P^{-1}(t)\tilde{\theta}(t) \tag{69}$$

Taking the time derivative of (69) we obtain:

$$\dot{V}(t) = \frac{1}{2}\tilde{\theta}^T(t)\frac{d}{dt}(P^{-1})\tilde{\theta}(t) + \tilde{\theta}^T P^{-1}(t)\dot{\tilde{\theta}}(t) \tag{70}$$

Using (67)-(68), one gets from (70) that:

$$\begin{aligned}\dot{V}(t) = &-s(t)\frac{\tilde{\theta}^T\Lambda_p^T}{1+||\Lambda_p^T\Lambda_p||^2}Z_p \\ &- \frac{\beta}{2}s(t)\tilde{\theta}^T(t)P^{-1}(t)\tilde{\theta}(t) - \frac{1}{2}s(t)\frac{\tilde{\theta}^T\Lambda_p^T\Lambda_p\tilde{\theta}}{1+||\Lambda_p^T\Lambda_p||^2}\end{aligned} \tag{71}$$

If $t < t_F$, by (65) we have $\dot{V}(t) = 0$: the Lyapunov function is non-increasing. When t become greater than t_F ($s(t) = 1$), we have by Theorem 1 that $Z_p \equiv 0$, then (71) becomes

$$\dot{V}(t) = -\beta V(t) - \frac{1}{2}\frac{\tilde{\theta}^T\Lambda_p^T\Lambda_p\tilde{\theta}}{1+||\Lambda_p^T\Lambda_p||^2} \leq -\beta V(t) \tag{72}$$

since the matrix $\Lambda_p^T\Lambda_p$ is positive semi-definite. As a result, for all $t \geq t_F$, there exists $K > 0$ such that $V(t) \leq Ke^{-\beta t}V(0)$ and $\tilde{\theta}$ is thus exponentially decaying to zero with a rate β : $\hat{\theta} \to \theta$ exponentially fast and the proof is complete.

3.5. Exponential stability of $E(x,t)$

In this section we prove the exponential stability of the error system $E(x,t)$, referring to the results in sections 3.2, 3.3 and 3.4.

Theorem 4. *Consider the error system (9)-(10) with boundary conditions (11) and initial conditions $\tilde{u}_0, \tilde{v}_0$ in $L^2[0,1]$, with observer gains $p_1(x)$ and $p_2(x)$ given in (41) and with feedback gains $m_1(x,t)$ and $m_2(x,t)$ given in (16) and (18). Under Theorems 1, 2 and 3 the error system is exponentially stable in the L^2 sense.*

PROOF. Using (14), one gets the following:

$$||E(.,t)||_{L^2[0,1]} \leq ||Z(.,t)||_{L^2[0,1]} + ||\Lambda(.,t)\tilde{\theta}(t)||_{L^2[0,1]} \tag{73}$$

By definition:

$$\begin{aligned}||\Lambda(,t)\tilde{\theta}(t)||^2_{L^2[0,1]} = &\int_0^1 (\lambda_{11}(x,t)\tilde{\theta}_1(t) + \lambda_{12}(x,t)\tilde{\theta}_2(t))^2 dx \\ &+ \int_0^1 (\lambda_{21}(x,t)\tilde{\theta}_1(t) + \lambda_{22}(x,t)\tilde{\theta}_2(t))^2 dx\end{aligned} \tag{74}$$

After expanding the squared parentheses in (74) and using basic identity inequalities we get:

$$\begin{aligned}||\Lambda(,t)\tilde{\theta}(t)||^2_{L^2[0,1]} \leq &\, 2\tilde{\theta_1}^2||\Lambda_1(.,t)||^2_{L^2[0,1]} \\ &+ 2\tilde{\theta_2}^2||\Lambda_2(.,t)||^2_{L^2[0,1]}\end{aligned} \tag{75}$$

Then, by Theorem 2, there exist two positive constants M_1 and M_2 such that:

$$\begin{aligned}||\Lambda(,t)\tilde{\theta}(t)||^2_{L^2[0,1]} &\leq 2M_1\tilde{\theta_1}^2 + 2M_2\tilde{\theta_2}^2 \\ &\leq \sqrt{M}||\tilde{\theta}(t)||_2\end{aligned} \tag{76}$$

where $M = max\{2M_1, 2M_2\}$. Considering (73) along with (76) we have:

$$||E(.,t)||_{L^2[0,1]} \leq ||Z(.,t)||_{L^2[0,1]} + \sqrt{M}||\tilde{\theta}(t)||_2 \tag{77}$$

Since $||Z(.,t)||_{L^2[0,1]}$ and $||\tilde{\theta}(t)||_2$ are exponentially decaying (referring to Theorem 1 and Theorem 3, respectively), then so is $||E(.,t)||_{L^2[0,1]}$.

4. Experimental Setup: Modeling and Process Description

We evaluate our observer on the TIF plant, a 15kW cooling system built at CERN to run educative experiments for developing and improving CO_2 cooling technology [31]. This refrigeration system is shown in Fig. 1 and schematically depicted in Fig. 2. It consists of a circulation system where the cold CO_2 refrigerant is pumped by the pump (LP3004) to the transfer lines (two concentric cylindrical tubes in vacuum isolation) and then heated by means of two heaters (EH7027 and EH7028) to provide the hot CO_2 refrigerant. Both hot and cold refrigerants exchange heat through the transfer lines, and finally the hot fluid is cooled down by the chiller (HX3082) to be pumped again into the cold line. The accumulator is used to set a desired output pressure at the hot side. We focus on the transfer line, as this part is particularly complex to model and necessitates an advanced observation scheme for distributed systems. The plant is equipped with four temperature sensors placed at the extremities of the tubes (shown in Fig. 2), which measure the input and output temperatures on both hot and cold sides. The control input is through the two heaters (EH7027 and EH7028), where we can vary the temperature of the hot input by adding and removing heat and thus create some transients in the system.

4.1. Modeling of the Heat Exchanger

We consider the concentric tubes heat exchanger schematically depicted in Fig. 3. This exchanger is a counter-flows heat exchanger, in which hot and cold fluids flow in opposite directions to maximize the heat transfer. Both the hot and the cold fluids enter in liquid phase and leave in liquid phase (no change of phase inside the exchanger). The flow of heat from the hot side to the cold

Figure 1: 15kW TIF plant at CERN

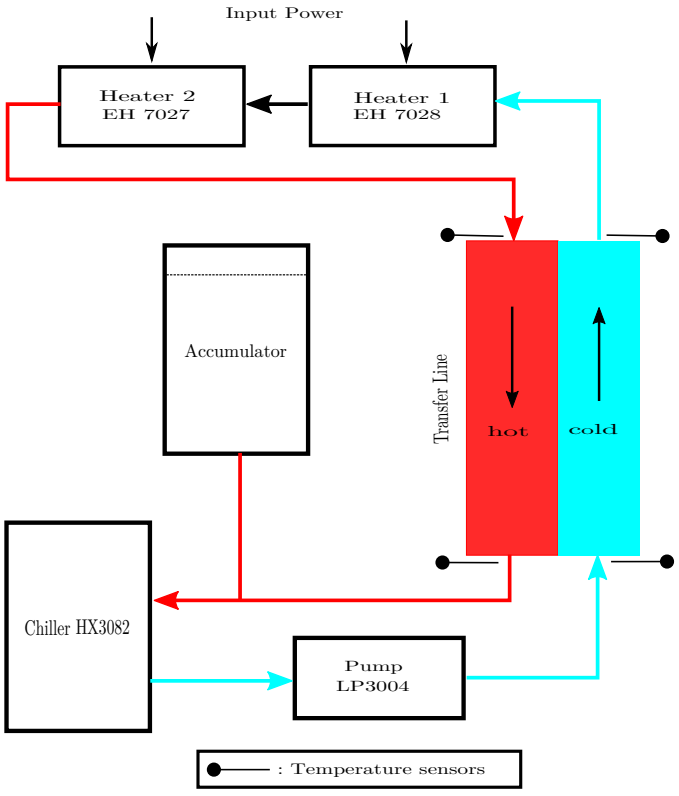

Figure 2: Schematic of the TIF plant

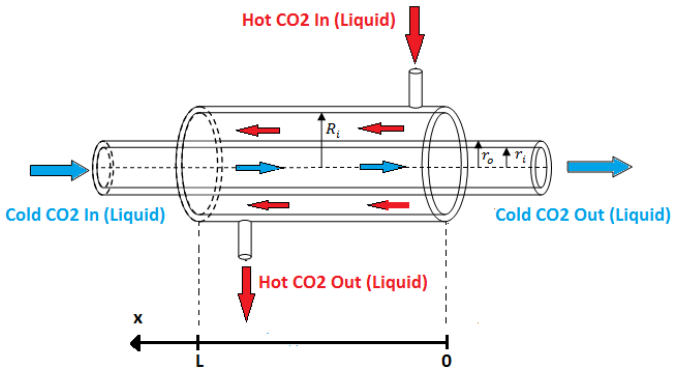

Figure 3: CO_2 single phase heat exchanger

Table 1: Definition of system variables and constants (SI units) k = C (cold fluid) or k = H (hot fluid)

Symbol	Description	Unit
L	Length of the exchanger	m
ρ^k	Density	kg/m^3
H^k	Specific Enthalpy	J/kg
$\dot{m}^k$	Mass flow rate	kg/s
T^k	Temperature	K
h	Heat transfer coefficient (HTC)	$W/m^2.K$
A^k	Tubes cross-sectional area	m^2
D_1	Inner tube diameter	m
C_P^k	Specific heat at constant pressure	$J/kg.K$

side is done through the wall interface.

The mathematical model is derived based on the following assumptions :

- the flow is 1-D unidirectional (the hot fluid flows in the positive x direction);
- the kinetic and potential energies of the flows entering and leaving the tubes are neglected;
- the wall thickness is neglected (no wall dynamics) and the heat transfer coefficient is uniform and quasi-steady i.e. using the classical "random walk" model, $\dot{h} = 0 + e(t)$ where $e(t)$ is a small white noise;
- the flow is considered incompressible; i.e. no significant change in density and equivalently in mass flow rate with time and along the length of the exchanger (only energy conservation equations are considered);
- in our working range of pressures and temperatures, we can assume a linear relation between enthalpy and temperature as follows:

$$H^H = C_P^H T^H, \qquad H^C = C_P^C T^C \tag{78}$$

where H^k is the specific enthalpy, T^k is the temperature and C_P^k is specific heat at constant pressure.
Under these assumptions, the 1D flow transport can be

described by a set of first order hyperbolic partial differential equations of balance laws (see e.g. [2]) as follows, $\forall x \in [0,1]$:

$$\partial_t T^H + c_1 \partial_x T^H = -K_1(T^H - T^C) \tag{79}$$

$$\partial_t T^C - c_2 \partial_x T^C = K_2(T^H - T^C) \tag{80}$$

where:

$$c_1 = \frac{\dot{m}^H}{LA^H\rho^H}, \quad c_2 = \frac{\dot{m}^C}{LA^C\rho^C}$$
$$K_1 = \frac{h\pi D_1}{A^H\rho^H C_P^H}, \quad K_2 = \frac{h\pi D_1}{A^C\rho^C C_P^C}$$

where ρ^k is the density, $\dot{m}^k$ is the mass flow rate, A^k is the tube surface area, D_1 is the inner tube diameter and h is the heat transfer coefficient. This system has boundary conditions:

$$T^H(0,t) = T^H_{in}(t) \qquad T^C(1,t) = T^C_{in}(t) \tag{81}$$

and initial conditions (assumed to be in $L^2[0,1]$):

$$T^H(x,0) = T^H_0(x), \qquad T^C(x,0) = T^C_0(x) \tag{82}$$

The problem of estimating $T^H(x,t)$ and $T^C(x,t)$ using boundary sensing is non-trivial because unknown parameters are present inside the domain (K_1 and K_2). For example, the heat transfer coefficient h (encapsulated in K_1 and K_2) affects the amount of energy transfered from the hot side to the cold side, and is usually estimated using correlations from physics (see e.g. [32]). The inaccurate estimation of h affects the accuracy of the estimation algorithm (as illustrated below in Section 4.4). In what follows, we consider online estimation of h together with the distributed states from the four measurements we have at the boundaries.

4.2. Reformulation as the general model of Section 2

The main difficulty induced by the dynamics (79)-(82) is that it involves a bilinear parametric nonlinearity i.e. the unknown parameter h multiples the unknown states $T^H(x,t)$ and $T^C(x,t)$. We decrease the level of complexity by augmenting the vector of states of the system from (T^H, T^C) to (T^H, T^C, h) with $\dot{h} = 0$. The augmented system is then linearized around the nominal system (T^H_N, T^C_N, h^N) given by:

$$\partial_t T^H_N + c_1 \partial_x T^H_N = -K_1^N(T^H_N - T^C_N) \tag{83}$$

$$\partial_t T^C_N - c_2 \partial_t T^C_N = K_2^N(T^H_N - T^C_N) \tag{84}$$

with boundary conditions:

$$T^H_N(0,t) = T^H_{in}(t), \qquad T^C_N(1,t) = T^C_{in}(t) \tag{85}$$

and initial conditions (assumed to be in $L^2[0,1]$):

$$T^H_N(x,0) = T^H_{N0}(x), \qquad T^C(x,0) = T^C_{N0}(x) \tag{86}$$

such that:

$$\begin{cases} T^H(x,t) &= T^H_N(x,t) + \Delta T^H(x,t), \\ T^C(x,t) &= T^C_N(x,t) + \Delta T^C(x,t), \\ h &= h^N + \Delta h, \end{cases} \tag{87}$$

where $\Delta T^H(x,t)$, $\Delta T^C(x,t)$ and Δh are perturbations around the nominal states. Using a Taylor expansion of order 1, one can obtain the dynamics of the perturbed states:

$$\begin{aligned} \partial_t \Delta T^H + c_1 \partial_x \Delta T^H = &-K_1^N(\Delta T^H - \Delta T^C) \\ &+\Delta h \frac{\pi D_1}{A^H\rho^H C_P^H}(-T^H_N + T^C_N) \end{aligned} \tag{88}$$

$$\begin{aligned} \partial_t \Delta T^C - c_2 \partial_x \Delta T^C = &K_2^N(\Delta T^H - \Delta T^C) \\ &+\Delta h \frac{\pi D_1}{A^C\rho^C C_P^C}(T^H_N - T^C_N) \end{aligned} \tag{89}$$

with boundary conditions:

$$\Delta T^H(0,t) = 0, \qquad \Delta T^C(1,t) = 0 \tag{90}$$

The initial conditions $\Delta T^H_0(x)$ and $\Delta T^C_0(x)$ are assumed to be in $L^2[0,1]$. Using a simple exponential transformation:

$$\Delta T^H_1 = e^{\frac{K_1^N}{c_1}x}\Delta T^H, \qquad \Delta T^C_1 = e^{-\frac{K_2^N}{c_2}x}\Delta T^C \tag{91}$$

The system (88)-(90) has exactly the same structure as the general model (1)-(3), with $u = \Delta T^H_1$, $v = \Delta T^C_1$, $\sigma_1(x) = K_1^N e^{(\frac{K_1^N}{c_1} + \frac{K_2^N}{c_2})x}$, $\sigma_2(x) = K_2^N e^{-(\frac{K_1^N}{c_1} + \frac{K_2^N}{c_2})x}$, $\phi_1(x,t) = \frac{\pi D_1 e^{\frac{-K_1^N}{c_1}x}}{A^H\rho^H C_P^H}(-T^H_N + T^C_N)$, $\phi_2(x,t) = \frac{\pi D_1 e^{\frac{K_2^N}{c_2}x}}{A^C\rho^C C_P^C}(T^H_N - T^C_N)$ and $\theta_1 = \theta_2 = \Delta h$.

Remark 4. *In practice and especially in heat exchanger networks, it is common to have a prior knowledge of the plant; e.g. ranges of pressures, ranges of temperatures, fluid speeds etc. This practical understanding of the system can help in deriving inaccurate estimates of the systems parameters, e.g. use correlations from the physics to calculate an estimate for the heat transfer coeffcient as in [32]. These estimates are considered as the nominal values for the exchanger parameters (c_1, c_2, K_1^N and K_2^N) and they are used in constructing the nominal model (83)-(86) along with $\phi_1(x,t)$ and $\phi_2(x,t)$. Hence, by knowing the operating point of the system and by measuring input/output temperatures, one can use our adaptive observer scheme to have an online estimation of the distributed states $T^H(x,t)$, $T^C(x,t)$ and also to recover the deviation of the heat transfer coefficient h from the correlation-based nominal value h^N.*

Remark 5. *Only the estimation of the heat transfer coefficient is considered in the evaluation process. This requires to remove the over-parameterization in system (1)-(3) by letting $\theta_1 = \theta_2 = \theta$, and as a consequence, the*

number of necessary swapping filters drops from four to only two. More precisely, the adaptive observer will be:

$$\begin{aligned}\partial_t\hat{u} + c_1\partial_x\hat{u} &= \sigma_1(x)\hat{v} + \hat{\theta}(t)\phi_1(x,t)\\ &\quad - p_1(x)(\hat{u}(1,t) - y_1(t)) + m_1(x,t)\\ \partial_t\hat{v} - c_2\partial_x\hat{v} &= \sigma_2(x)\hat{u} + \hat{\theta}(t)\phi_2(x,t)\\ &\quad - p_2(x)(\hat{u}(1,t) - y_1(t)) + m_2(x,t)\end{aligned}$$

$$\begin{aligned}\hat{u}(0,t) &= U(t) + q(\hat{v}(0,t) - y_2(t))\\ \hat{v}(1,t) &= V(t)\end{aligned}$$

The swapping filters are

$$\partial_t\lambda_1 + c_1\partial_x\lambda_1 = \sigma_1(x)\lambda_2 - p_1(x)\lambda_1(1,t) + \phi_1(x,t)$$

$$\partial_t\lambda_2 - c_2\partial_x\lambda_2 = \sigma_2(x)\lambda_1 - p_2(x)\lambda_1(1,t) + \phi_2(x,t)$$

$$\lambda_1(0,t) = q\lambda_2(0,t), \quad \lambda_2(1,t) = 0$$

with $m_1(x,t) = -\lambda_1(x,t)\dot{\hat{\theta}}$ *and* $m_2(x,t) = -\lambda_2(x,t)\dot{\hat{\theta}}$. $\hat{\theta}(t)$ *is calculated using the adaptive law (63)-(65) but with* $\Lambda_p(t) = [\lambda_1(1,t), \lambda_2(0,t)]$ *instead of (26). Furthermore, there is no change in the calculation of* $p_1(x)$ *and* $p_2(x)$ *as equation (41) is used.*

4.3. In-domain evaluation of the observer through simulations

As shown in Fig.2, temperatures can only be measured at the extremities of the tubes using four input/output temperature sensors. Hence, we can't validate experimentally the distributed state estimation because we can't take measurements from inside the domain. However, we evaluate the estimation of temperatures inside the domain through numerical simulations. In this section, we also discuss the effect of linearization done in Section 4.2.
First of all, assume that the model (79)-(82) represents the real dynamics of the exchanger under study. We have built our own simulator to simulate (79)-(82). The simulator implements a finite difference scheme of second order accuracy for the space derivatives, and ode15s (Matlab) for the time derivatives. The kernel equations (35)-(40) are solved by a method called successive approximations [13]. The main idea of this method is to write the set of PDEs (35)-(40) in the integral form using the method of characteristics. Afterwards, the integral equations are solved using recursion up to an order of accuracy defined by the user (see [13] for more details). Since the observer is not built directly on system (79)-(82) but on the linearized version (88)-(90), we expect the quality of the estimation to be better when the nominal model (83)-(86) is chosen close to the real system. The simulations are done in the following order:

1. Simulate system (79)-(82) with real measured inputs (see section 4.4) and assume that the real heat transfer coefficient is $h_{real} = 290$. We then consider the obtained temperatures $T^H_{real}(x,t)$ and $T^C_{real}(x,t)$ as the real distributed temperatures of exchanger.
2. Use $T^H_{real}(1,t)$ and $T^C_{real}(0,t)$ as the real boundary measurements
3. Simulate the observer scheme starting with nominal heat transfer coefficient $h^N_1 = 180$, $h^N_2 = 230$ and $h^N_3 = 250$.
4. Compute the estimation $\hat{T}(x,t) = T^N(x,t) + \Delta\hat{T}(x,t)$ and the estimation error $E(x,t) = |T_{real}(x,t) - \hat{T}(x,t)|$ on both hot and cold sides.

In order to choose different operating points, we vary the nominal heat transfer coefficients; e.g. $h^N_1 = 180$ corresponds to a far operating point (since $h_{real} = 290$) and so on. The results of the steady state estimation errors are shown in Fig.4. A first important remark is that the estimation error inside the domain is greater than that at the boundaries for all the operating points. A glimpse on the observer design can actually give us the reason. Considering the linear case, the adaptation law uses only boundary outputs to estimate the parameters. If the outputs are informative enough, the estimated values of the parameters will converge to the real ones when the outputs agree. Since the observer is of Luenberger type and its stability is guaranteed by the observer gains $p_1(x)$ and $p_2(x)$, the in-domain estimates should also converge. When considering the real system, the adaptation law ensures the convergence of the boundary outputs, but this does not necessarily imply an in-domain convergence since the observer is built on the linearized version of the system and not on the real plant. We can see from Fig.4 that as the nominal model approaches the real model (i.e. h^N approaches h_{real}), the estimation error in the domain is decreased. By looking into the order of error magnitude, we find that the maximum absolute estimation error on both sides is less than 0.018 K in the hole domain. This is significantly a negligible in-domain estimation error. We can then reasonably deduce that the effect of linearization is almost negligible and does not affect the quality of the in-domain estimation. The reason is mainly because the bilinear parameter nonlinearity ($K_1(T^H - T^C)$) encountered in the plant is not a strong nonlinearity.

We now show the time series of the heat transfer coefficient on Fig.5. We can see that the estimations from the three different nominal operating points stabilize at steady states that do not correspond to $h_{real} = 290$. The reason is clearly the linearization, since when the nominal operating point is chosen close to the system's real operating point, the estimation is improved. This is more significant if we compute the relative steady state error: $RSE(\%) = \frac{|h_{real} - \hat{h}_{steady}|}{h_{real}} * 100$ for each operating point.

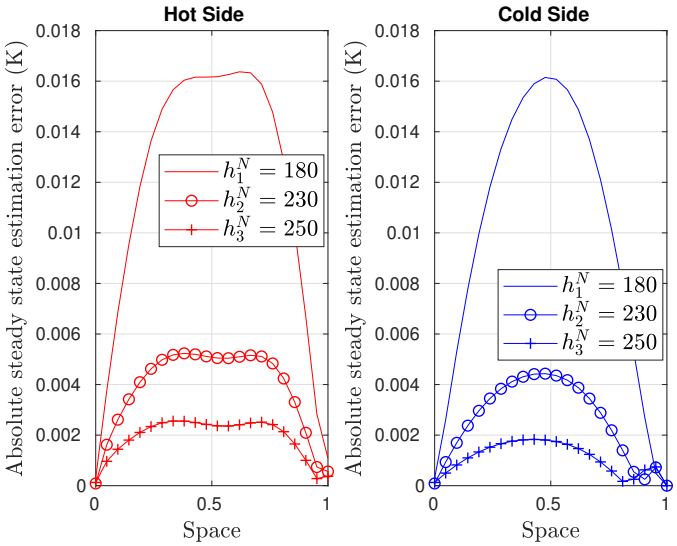

Figure 4: Steady state error on the distributed temperature profiles for three different operating points

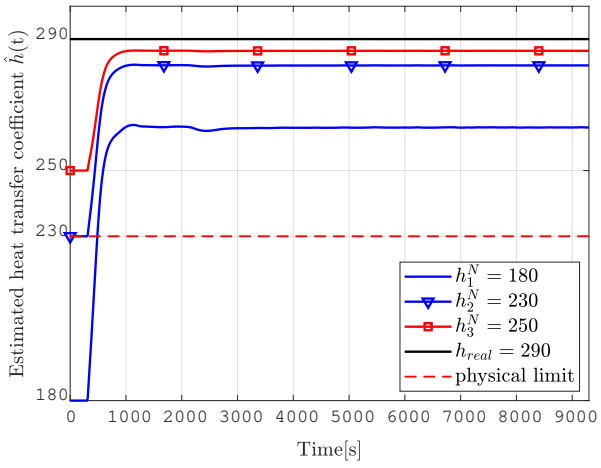

Figure 5: Estimated heat transfer coefficient $\hat{h}(t)$ for three different operating points

Table 2: RSE for three different operating points

Operating point	RSE (%)
$h_1^N = 180$	9.31
$h_2^N = 230$	2.79
$h_3^N = 250$	1.24

The RSE decreases when h^N approaches h_{real} as shown in Table 2 and its magnitude is less than 10% even for a very far operating point (i.e. $h^N = 180$). It is also important to mention that there is always a physical limit on the chosen values of the operating point h^N (see Fig.5). This limit is calculated using thermodynamical correlations [30]. For the exchanger under study, the minimal calculated physical limit is $h^N = 230$, and we can notice on Table 2 that the corresponding RSE is less than 3%. This is considered very small, and we can conclude that in the physical working ranges of the exchanger, the effect of linearization on the estimation of the heat transfer coefficient is reasonably small.

4.3.1. Comparison with literature observers

Previously, several boundary observer designs for hyperbolic systems relying on an exact knowledge of the parameters of the system have been designed. We intend to show the importance of the adaptive design in the case where the nominal parameters differ from the real ones as this is the main problem that we faced while designing an observer for our experiment. To compare our results we choose two designs already present in the literature: the Lyapunov-based observer proposed in [18] and the two-sided backstepping observer from [14].

We simulate the observers proposed in [18] and [14] at the three different operating points ($h_1^N = 180$, $h_2^N = 230$, and $h_3^N = 250$), following exactly the procedure explained in Section 4.3 (steps 1 to 3). We recall that the observer designs in [18] and [14] are built directly using the nominal parameters of the system. The main objective of the comparison is to check if the parameter adaptation improves the accuracy of the temperature estimates.

We simulate the three observers with real measured inputs (see Section 4.4) starting with the same initial conditions. We have calculated the L^1 norm of the estimation error on both hot and cold sides for the three different operating points:

$$||\epsilon^K(t)||_{L^1[0,1]} = \int_0^1 |T^K_{real}(x,t) - \hat{T}^K(x,t)|dx \qquad (92)$$

The results are shown on Fig.6. We can observe that in all the plots the estimation error using the adaptive design is always less than that resulting from the observers in [18] and [14]. The adaptive observer significantly ameliorates the estimation in transient states and contributes to nearly 1K temperature improvement at steady states.

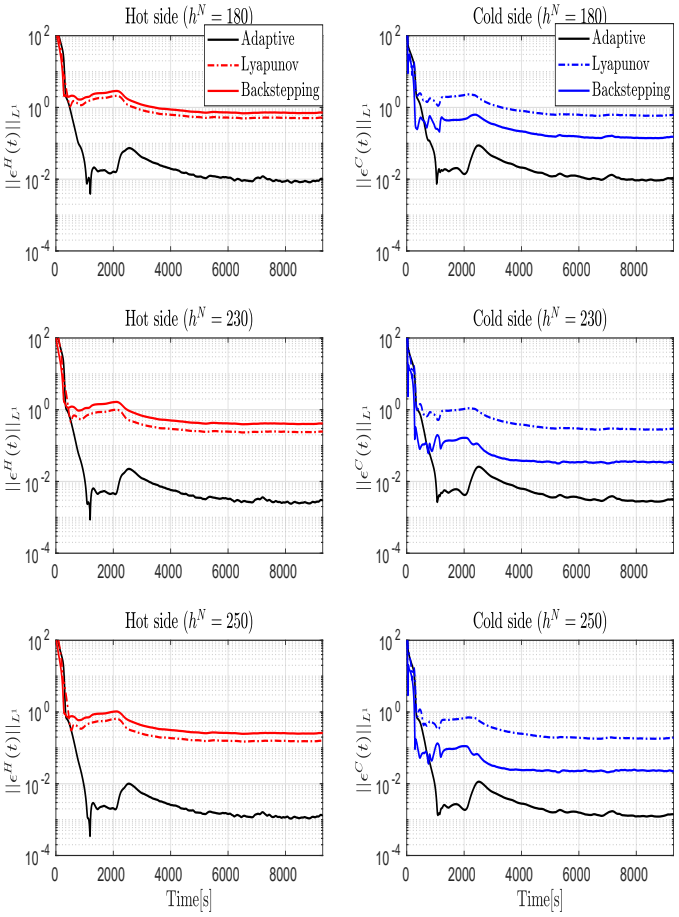

Figure 6: Comparison of the L^1 estimation error resulting from three different methods for three different operating points

Table 3: Heating power modulation

Variation	Time(s)
increase	0(s)
decrease	479(s)
increase	800(s)
increase	1391(s)
decrease	2050(s)

These estimation enhancements provided by the parameter adaptation are very important to the designers of the CO_2 cooling technology at CERN, since they work with highly accurate temperature sensors.

4.4. Experimental evaluation of the observer

Once the system has reached a steady state and liquid CO_2 starts circulating in all parts of the TIF plant, the experiment is done by modulating the input heating power by several increases and decreases at different instants in time as shown in Table 3, thus inducing system transients and exciting the system frequencies. Keeping in mind that we have only one parameter to estimate, which is the heat transfer coefficient, the input in Table 3 is considered sufficiently persistently exciting. The temperature is measured by the four sensors schematically depicted on Fig.2. They are PT100 RTD sensors. In particular, they are "in-flow" sensors, i.e., they are mounted inside the tube to measure the temperature of the refrigerant itself, instead of being glued to the top of the tube. These PT100s output a resistance to a "Conditioner" which is an object that converts the resistance signal into a 4-20 mA input for the PLC. The PLC then has a range that determines what the minimum (4mA) and maximum (20mA) values for that particular sensor are, and uses this to convert the 4-20 mA signal into a degree Celsius (C) value. On the computer, we have a SCADA system called WinCCOA, which exchanges signals from the PLC and displays it for the user. From the WinccOA interface, we are able to export the data to a CSV file. We import the data into Matlab where we make all the analysis. The observer schemes are not implemented directly on the real plant. The experimental evaluation of the observers is done in Matlab using the real data collected in the CSV files.

The TIF plant is 17.665 m long ($L = 17.665\,\mathrm{m}$) with cross-sectional areas $A^H = 7.6306 \times 10^{-4}\,\mathrm{m}^2$, $A^C = 1.131 \times 10^{-4}\,\mathrm{m}^2$. During this experiment, the exchanger is operating in the liquid phase and in the following working ranges: pressure between [5 MPa, 6 MPa], temperatures between [253 K, 288 K] and mass flow rates close to 0.047 Kg/s. With these given information, one can use the equation of state (EoS) for CO_2 [33] with the correlation in [32] to calculate the nominal values for the exchanger parameters. We found: $c_1 = 0.0237\,\mathrm{s}^{-1}$, $c_2 = 0.0037\,\mathrm{s}^{-1}$, $K_1^N = 0.0051\,\mathrm{s}^{-1}$ and $K_2^N = 0.0351\,\mathrm{s}^{-1}$. The computed nominal heat transfer coefficient is $h^N = 230\,\mathrm{W/m^2.K}$. Afterwards, the nominal model (83)-(86) is simulated with

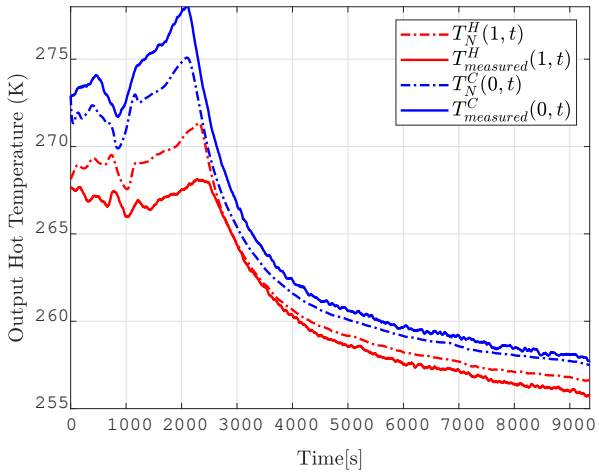

Figure 7: Comparison between the reference model and experiments

the measured inputs. By comparing the temperature outputs of the nominal model ($T_N^H(1,t)$ and $T_N^C(0,t)$) and the experimental measures on Fig.7, one can notice that the nominal model captures the main dynamics of the real system. However, the temperatures predicted by the model involve a temperature shift and this shift changes with time. We know from the physics that the heat transfer coefficient is the parameter responsible for this shift in temperature magnitudes, since it affects the amount of energy transfered from the hot side to the cold side. One can then draw two conclusions: first the linear system (79)-(82) represents a good physical model for the exchanger, second the real heat transfer coefficient is time -varying. In fact, the dynamics of h are very complex since h can vary with the variation of many physical quantities and especially temperature. In our adaptive design, we have assumed that h is quasi-steady (see the modeling assumptions list in Section 4.1). Doing so, we intend to use the parameter adaptation algorithm to recover the values of the heat transfer coefficient in the intervals were we have slow variations in temperature (as we will show later in the analysis).

As the nominal operating point is settled, we can proceed to the estimation part. Since we can't take measurements from inside the domain, we evaluate our theoretical results against the output sensor measurements. We start all observers with the same initial condition.
Fig.8 shows the temperatures estimated by the three observers along with the experimental measurements. One can notice that the quality of the estimation is better using our proposed adaptive estimator during both transient and steady states. The estimation error magnitude on both hot and cold sides is presented on Fig.9. Note that the error is decreased by nearly 5K during the transient phase and 1K

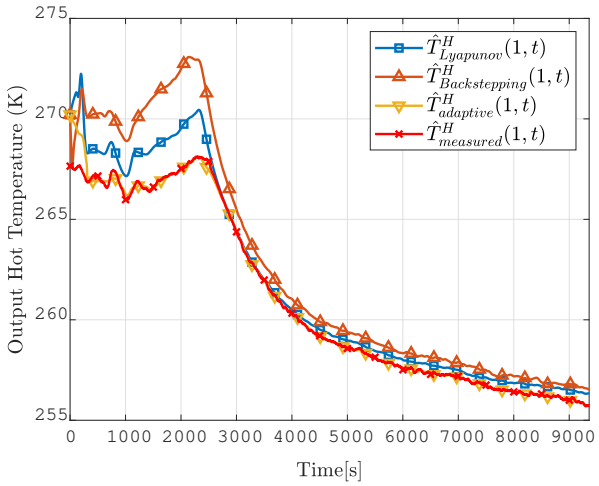

(a) Hot fluid temperature.

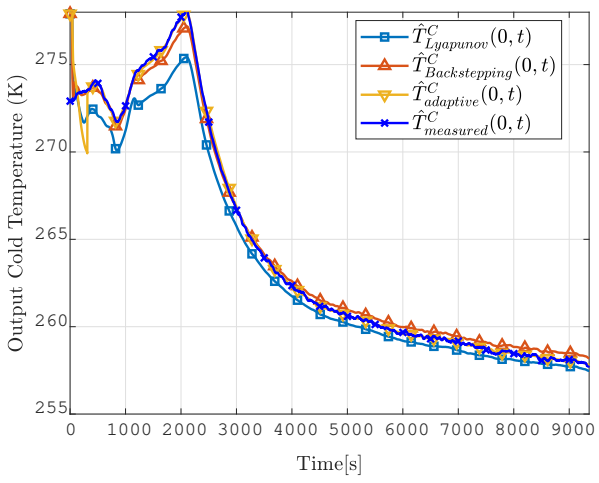

(b) Cold fluid temperature.

Figure 8: Temperature trends estimated with three different methods.

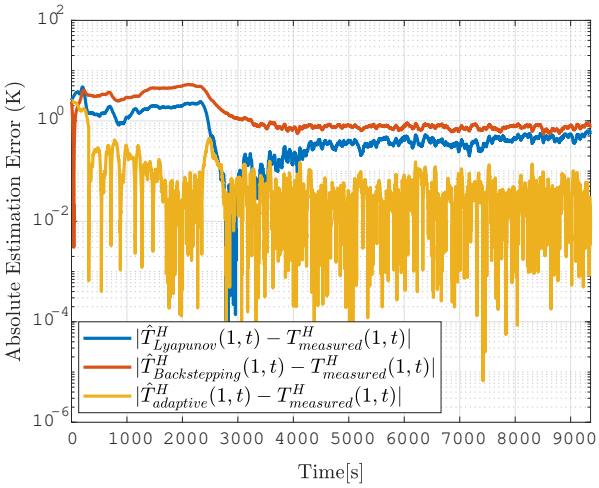

(a) Output hot estimation errors.

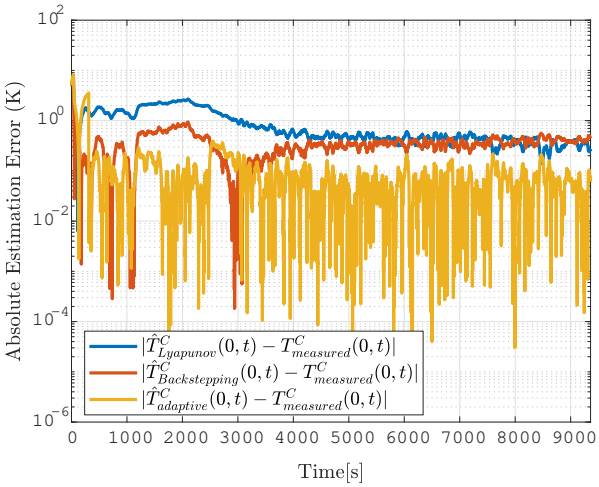

(b) Output cold estimation errors.

Figure 9: Output estimation errors of the three different observations methods.

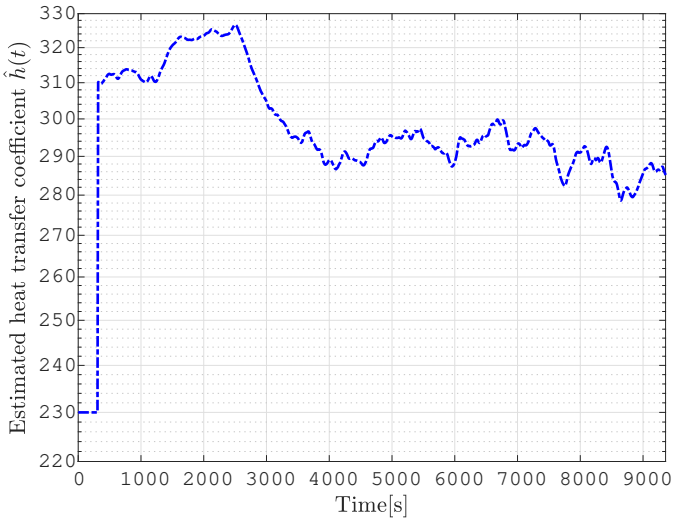

Figure 10: Estimated heat transfer coefficient $\hat{h}(t)$

in the steady state, using the adaptive estimator. The estimations using the two other designs (Lyapunov and two-sided backstepping observers) are comparable and with an accuracy limited by their assumption of a perfect knowledge of the system's parameters. Considering a negligible contribution of the linearization error as illustrated in Section 4.3., we can conclude that the adaptive observer can estimate the distributed state with enough degree of accuracy.

The estimation of the heat transfer coefficient is shown on Fig.10: the estimation starts at the nominal value $h^N = 230$ and then after the time $t_F = \frac{1}{c_1} + \frac{1}{c_2} = 310.54\,\text{s}$ the adaptation law starts functioning. Since we have implicitly assumed that h is quasi-steady, we expect the estimated heat transfer coefficient to converge to different steady states at different intervals of time. We can infer from Fig.10 approximately three different values of the heat transfer coefficient in three different time intervals: $h \approx 312$ for t $\in$ [310s,1235s], $h \approx 325$ for t $\in$ [1625s,2530s] and $h \approx 295$ for t $\in$ [3550s,8400s].

5. Conclusion

We have developed an adaptive observer that estimates unknown parameters inside the domain for 2 by 2 first order 1-D hyperbolic PDEs. The observer is based on a swapping design, which allows us to write the estimation error on the states as a static linear combination of the estimation error on the parameters. Standard backstepping and parameter estimation techniques can then be used. We thus proved boundedness of regressors filters and obtained sufficient conditions to ensure the exponential convergence of the estimation errors. The designed observer uses only boundary sensing, and allows one to estimate the full distributed states. Our method is evaluated experimentally on the TIF refrigeration system at CERN,

and our results show that the adaptive observer captures the main dynamics of the real system. For future works, it would be interesting to consider the bilinear parameterization directly in (79)-(82), i.e. to estimate h and $T^H(x,t)$, $T^C(x,t)$ directly without passing through the linearization step, using boundary sensing only.

6. Acknowledgment

The authors are grateful to Benjamin Bradu (CERN) for his insights on the heat exchanger process and model. This work was sponsored within the ITEA3 European project, 15016 EMPHYSIS (Embedded systems with physical models in the production code software).

References

[1] B. Verlaat, M. Van Beuzekom, A. Van Lysebetten, CO2 cooling for HEP experiments, in: Topical Workshop on Electronics for Particle Physics (TWEPP-2008), Naxos, Greece, 2008, pp. 328–336.

[2] C.-Z. Xu, G. Sallet, Exponential stability and transfer functions of processes governed by symmetric hyperbolic systems, ESAIM: Control, Optimisation and Calculus of Variations 7 (2002) 421–442.

[3] P. Goatin, The aw–rascle vehicular traffic flow model with phase transitions, Mathematical and computer modelling 44 (3-4) (2006) 287–303.

[4] M. Gugat, M. Dick, Time-delayed boundary feedback stabilization of the isothermal euler equations with friction, Math. Control Relat. Fields 1 (4) (2011) 469–491.

[5] J.-M. Coron, B. d'Andrea Novel, G. Bastin, A lyapunov approach to control irrigation canals modeled by saint-venant equations, in: IEEE European Control Conference (ECC), 1999, pp. 3178–3183.

[6] C. Curro, D. Fusco, N. Manganaro, A reduction procedure for generalized Riemann problems with application to nonlinear transmission lines, Journal of Physics A: Mathematical and Theoretical 44 (33) (2011) 335205.

[7] F. Di Meglio, Dynamics and control of slugging in oil production, Ph.D. thesis, École Nationale Supérieure des Mines de Paris (2011).

[8] J. Rauch, M. Taylor, R. Phillips, Exponential decay of solutions to hyperbolic equations in bounded domains, Indiana university Mathematics journal 24 (1) (1974) 79–86.

[9] D. L. Russell, Controllability and stabilizability theory for linear partial differential equations: recent progress and open questions, SIAM Review 20 (4) (1978) 639–739.

[10] F. Castillo, E. Witrant, C. Prieur, L. Dugard, Dynamic boundary stabilization of linear and quasi-linear hyperbolic systems, in: 51st Annual Conference on Decision and Control (CDC), IEEE, 2012, pp. 2952–2957.

[11] G. Bastin, J.-M. Coron, Stability and boundary stabilization of 1-d hyperbolic systems, Vol. 88, Springer, 2016.

[12] R. Vazquez, M. Krstic, J.-M. Coron, Backstepping boundary stabilization and state estimation of a 2× 2 linear hyperbolic system, in: 50th IEEE Conference on Decision and Control and European Control Conference (CDC-ECC), 2011, pp. 4937–4942.

[13] L. Hu, F. Di Meglio, R. Vazquez, M. Krstic, Control of homodirectional and general heterodirectional linear coupled hyperbolic PDEs, IEEE Transactions on Automatic Control 61 (11) (2016) 3301–3314.

[14] J. Auriol, F. Di Meglio, Two-sided boundary stabilization of heterodirectional linear coupled hyperbolic pdes, IEEE Transactions on Automatic Control 63 (8) (2017) 2421–2436.

[15] P. Bernard, M. Krstic, Adaptive output-feedback stabilization of non-local hyperbolic PDEs, Automatica 50 (10) (2014) 2692–2699.

[16] H. Anfinsen, O. M. Aamo, Adaptive output-feedback stabilization of linear 2× 2 hyperbolic systems using anti-collocated sensing and control, Systems & Control Letters 104 (2017) 86–94.

[17] F. Castillo, E. Witrant, C. Prieur, L. Dugard, Boundary observers for linear and quasi-linear hyperbolic systems with application to flow control, Automatica 49 (11) (2013) 3180–3188.

[18] F. Zobiri, E. Witrant, F. Bonne, PDE observer design for counter-current heat flows in a heat-exchanger, IFAC-PapersOnLine 50 (1) (2017) 7127–7132.

[19] A. Smyshlyaev, M. Krstic, Adaptive control of parabolic PDEs, Princeton University Press, 2010.

[20] F. Di Meglio, D. Bresch-Pietri, U. J. F. Aarsnes, An adaptive observer for hyperbolic systems with application to underbalanced drilling, IFAC Proceedings Volumes 47 (3) (2014) 11391–11397.

[21] M. Bin, F. Di Meglio, Boundary estimation of boundary parameters for linear hyperbolic PDEs, IEEE Transactions on Automatic Control 62 (8) (2017) 3890–3904.

[22] O. M. Aamo, Disturbance rejection in 2 x 2 linear hyperbolic systems, IEEE Transactions on Automatic Control 58 (5) (2013) 1095–1106.

[23] O. M. Aamo, Leak detection, size estimation and localization in pipe flows, IEEE Transactions on Automatic Control 61 (1) (2016) 246–251.

[24] M. Krstic, I. Kanellakopoulos, V.Petar, Nonlinear and adaptive control design, Wiley New York, 1995.

[25] G. Kreisselmeier, Adaptive observers with exponential rate of convergence, IEEE transactions on automatic control 22 (1) (1977) 2–8.

[26] H. Anfinsen, M. Diagne, O. M. Aamo, M. Krstic, An adaptive observer design for $n + 1$ coupled linear hyperbolic pdes based on swapping, IEEE Transactions on Automatic Control 61 (12) (2016) 3979–3990.

[27] H. Anfinsen, M. Diagne, O. M. Aamo, M. Krstic, Estimation of boundary parameters in general heterodirectional linear hyperbolic systems, Automatica 79 (2017) 185–197.

[28] H. Anfinsen, F. Di Meglio, O. M. Aamo, Estimating the left boundary condition of coupled 1-D linear hyperbolic PDEs from right boundary sensing, in: IEEE European Control Conference (ECC), 2016, pp. 2179–2184.

[29] T. Ahmed-Ali, F. Giri, M. Krstic, L. Burlion, F. Lamnabhi-Lagarrigue, Adaptive boundary observer for parabolic PDEs subject to domain and boundary parameter uncertainties, Automatica 72 (2016) 115–122.

[30] P. A. Ioannou, J. Sun, Robust adaptive control, Vol. 1, PTR Prentice-Hall Upper Saddle River, NJ, 1996.

[31] T. Paola, P. Petagna, S. Pavis, J. Godlewski, J. Daguin, H. Postema, M. Ostrega, Design, construction and commissioning of a 15 kW CO2 evaporative cooling system for particle physics detectors: lessons learnt and perspectives for further development, in: Proceedings of Science (PoS), 2014, p. 213.

[32] V. Gnielinski, New equations for heat and mass transfer in turbulent pipe and channel flow, Int. Chem. Eng. 16 (2) (1976) 359–368.

[33] I. H. Bell, J. Wronski, S. Quoilin, V. Lemort, Pure and pseudo-pure fluid thermophysical property evaluation and the open-source thermophysical property library coolprop, Industrial & engineering chemistry research 53 (6) (2014) 2498–2508.